Self-assembled monolayers induced inter-conversion of crystal structure by vertical to lateral growth of aluminium doped zinc oxide thin films†

Yian Tai,* Jadab Sharma, Hsuan-Chun Chang, Thieu Vo Thi Tien and Yi-Shiang Chiou

Received 2nd September 2010, Accepted 18th November 2010
DOI: 10.1039/c0cc03607b

In this communication, we demonstrate the inter-conversion of crystal structure of aluminium doped zinc oxide (AZO) thin films from highly (002) plane oriented vertical growth to (103) plane oriented lateral growth by adjusting the polarity of the self-assembled monolayers (SAMs) on glass substrates at room temperature.

Transparent conducting oxide (TCO) thin films have received extensive research interest due to their versatile applications in electronic devices and solar cells.[1–3] Whilst tin doped indium oxide (ITO) is the most commonly used TCO, aluminium doped zinc oxide (AZO) has been the current choice due to the low cost and non-toxic properties.[3,4] AZO films are wide band gap semiconductors (E_g = 3.4–3.9 eV) having good electrical properties and high optical transmission in the visible and near-infrared (IR) regions.[2] Several methods have been developed for the fabrication of AZO films and a good quality material is obtained when either the deposition or the post-synthesis annealing temperature of the substrate is raised to above 100 °C.[2,4–7] This temperature requirement is not suitable for many of the recent devices due to the heat sensitivity of substrates used in the fabrication.[8] To avoid such difficulties, plasma sputtering techniques have been developed for the low temperature deposition, enabling fabrication of TCO films on a variety of substrates.[9] However, low temperature deposition yields amorphous materials with high resistivity indicating no direct control on crystal growth by gas phase deposition methods, which severely affects their performances.[6,8]

Recently, a self-assembled monolayer (SAM) technique has been applied to improve the quality of thin films at ambient conditions.[10] The SAM technique provides a unique opportunity to manipulate the physical and chemical properties of surfaces on a variety of substrates including SAMs on various TCOs.[11] As a result of change in surface energy, crystal growth on SAM functionalized surfaces can also be controlled, exhibiting an excellent nucleation site for different crystals. For example, several studies have been successfully carried out on ω-functionalized SAMs in a wet chemical environment to grow ceramic thin films with controlled crystalline structures.[12] Despite several such remarkable achievements having been reported, the full potential of SAMs on gas-phase crystal growth has never been explored. In this communication, we report the inter-conversion of crystal structure of aluminium doped zinc oxide (AZO) thin films by changing the polarity of SAMs at ambient conditions.

To understand the role of SAM in gas-phase crystal growth, three different SAMs were fabricated on glass substrates with positive (3-aminopropyltriethoxysilane, H_2N–SAM) and negative [(3,3,3-trifluoropropyl) trimethoxysilane, F_3C–SAM] partial charges and a molecule with no partial charge (*n*-propyltriethoxysilane, H_3C–SAM). AZO films were then deposited onto SAM modified glass substrates at room temperature using a deposition unit with RF magnetron sputtering from ceramic targets with a very low plasma power of 40 W.[13] Crystal structures of various AZO films were investigated by X-ray diffraction (XRD). It has been reported earlier that XRD patterns of AZO films at different dopant concentrations exhibit a predominant (002) peak of the ZnO hexagonal (wurtzite) structure, which indicate a preferential (002) orientated vertical growth with the *c*-axis perpendicular to the substrate surface.[14] However, a transition to lateral growth at 250 °C with a sharp increase in the (103) peak has also been reported recently.[15]

Fig. 1 shows (a) XRD patterns of AZO films (thickness, $t \approx 920$ nm) deposited on various SAM modified glass substrates, (b) plot of % intensity ratio of (002) to (103) peaks from the XRD patterns for different AZO films, reflection high-energy electron diffraction (RHEED) patterns of AZO films ($t \approx 720$ nm) deposited on (c) bare glass and (d) F_3C–SAM modified glass substrates. A clear variation in the crystal structure of AZO films on different substrates is evident

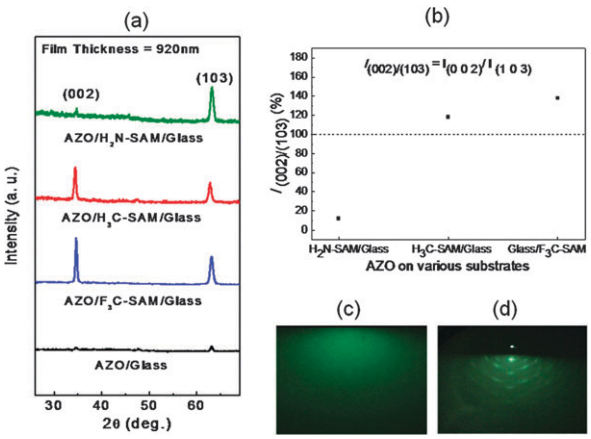

Fig. 1 (a) XRD patterns of AZO films ($t \approx 920$ nm) deposited on different SAM modified glass substrates, (b) plot of % intensity ratio of (002) to (103) peaks from the XRD patterns for different AZO films, RHEED patterns of AZO films ($t \approx 720$ nm) deposited on (c) bare glass and (d) F_3C–SAM modified glass substrates. AZO films were deposited at room temperature.

Department of Chemical Engineering, National Taiwan University of Science and Technology, 43 Keelung Rd., Sec. 4, Taipei-106, Taiwan. E-mail: ytai@mail.ntust.edu.tw; Fax: +886 2 2737 6644; Tel: +886 2 2737 6620

† Electronic supplementary information (ESI) available: Experimental details and additional data (contact angle, surface tension, XRD, RHEED, SEM, and XP spectra). See DOI: 10.1039/c0cc03607b

from the XRD patterns (Fig. 1a). For instance, the AZO film deposited on a bare glass substrate shows negligible signals from (002) and (103) crystal planes indicating formation of an amorphous film. However, crystallinity of AZO films improves significantly when deposited on SAM modified glass substrates but with a clear variation in the crystallographic orientation. For instance, the XRD pattern for an AZO film deposited on a glass substrate with a strong electron donating functional group (H_2N–SAM) shows a predominant (103) peak suggesting the lateral growth. A very weak (002) peak is also observed but the (002) to (103) peak intensity ratio ($I_{(002)/(103)}$) is negligible (0.1). In sharp contrast, the growth pattern is switched to the vertical mode when the AZO film is deposited on a glass substrate with a strong electron withdrawing group (F_3C–SAM). The XRD pattern of such a film shows a predominant (002) peak, with a significantly high $I_{(002)/(103)}$ of 13.8. Similarly, the crystal structure of the AZO film deposited on a neutral SAM substrate (H_3C–SAM) exhibits an intermediate behavior ($I_{(002)/(103)}$ = 11.8). The variation of crystal growth behavior is also clear from the plot of % intensity ratio of (002) to (103) peaks as shown in Fig. 1b for various AZO films.

In addition, a little shift in the (002) peak position is also observed indicating the lattice stress due to the Al doping. In general, XRD of crystalline ZnO films grown at >150 °C shows a (002) peak at $2\theta \approx 34.2°$.[16] A positive shift of the (002) peak is expected when few or all of the Zn^{2+} (ionic radii, r = 72 pm) ions are replaced by Al^{3+} (r = 53 pm) due to the mismatch of ionic radii.[13,16] Positive shifts of 0.3° and 0.4° are observed for AZO films deposited on F_3C–SAM and H_2N–SAM modified glass substrates, respectively. However, shift in the (002) peak position is only ~0.19° for the AZO film deposited on a H_3C–SAM modified glass substrate. This indicates that most of the Al atoms are substituted in the Zn sites for the former case, while majority of Al atoms are merely present in the interstitial sites for the AZO film on the H_3C–SAM modified glass substrate.[13] Similarly, an increase in the full width at half-maximum (FWHM) of (002) or (103) peak corresponds to the decrease in grain size or vice versa. When FWHM becomes smaller grain size of the film increases indicating the improvement of the crystallinity with lesser defects in the film.[17] FWHM of 0.23° is observed for both the AZO films deposited on F_3C–SAM and H_3C–SAM modified glass substrates, respectively. As expected, the RHEED profile of an AZO film deposited on a bare glass substrate at room temperature is featureless (Fig. 1c), while the profile for the AZO film deposited on a SAM modified substrate (*e.g.*, F_3C–SAM) shows arrays of diffraction spots characteristic of a polycrystalline thin film (Fig. 1d).

A good correlation between the normalized (002) peak intensity ($I_{(002)}$) and the abundance of $–CF_3$ and $–NH_2$ groups on the surface is revealed from the XRD studies on various AZO films by systematically varying the mixing ratio of the corresponding SAM forming molecules. For example, Fig. 2a shows the XRD patterns of AZO films deposited on various glass substrates with increasing ratio of $–CF_3$ to $–NH_2$ groups (estimated from X-ray photoelectron spectra, XPS). As we move from the pure H_2N–SAM to pure F_3C–SAM, $I_{(002)}$ also increases from 0.1 to 1. It is noteworthy to mention that when

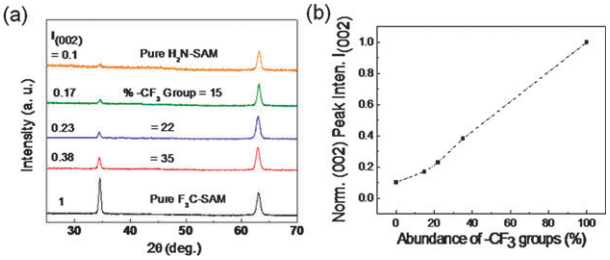

Fig. 2 (a) XRD patterns of AZO films deposited on various glass substrates with an increasing ratio of $–CF_3$ to $–NH_2$ groups (estimated from XPS). (b) Plot of normalized intensity of the (002) peak against the % CF_3–SAMs. (002) Peaks were normalized with the (002) peak of the AZO film deposited on the F_3C–SAM modified glass substrate.

the coverage of F_3C–SAM is varied from 15% to 35%, $I_{(002)}$ also varies from 0.17 to 0.38. The plot of normalized intensity of the (002) peak against the % CF_3–SAMs is given in Fig. 2b. Since enhancement of the (002) peak intensity indicates a predominant vertical growth, the above results unambiguously indicate a transition from the lateral to vertical growth at higher abundance of $–CF_3$ over $–NH_2$ groups. In essence, this allows us to modulate the crystal structure of AZO films simply by manipulating the mixing ratio of the respective SAM forming molecules. Surprisingly, shift in the (002) peak position varies from ~0.27° to ~0.4° with the gradual increase in % $–NH_2$ groups; this is in good agreement with the trend discussed in the preceding section.

Fig. 3 shows scanning electron micrographs (SEM) of AZO films deposited on various substrates ($t \approx$ 120 nm). In particular, the AZO film on a bare glass substrate shows amorphous behavior (Fig. 3a). The grains have a tendency to decrease in size when AZO is deposited on a F_3C–SAM modified glass substrate (Fig. 3b), while they grow much larger in size when deposited on a H_2N–SAM modified glass substrate (Fig. 3d). An intermediate behavior is observed for the AZO film deposited on a H_3C–SAM modified glass substrate (Fig. 3c). This is in good agreement with the XRD

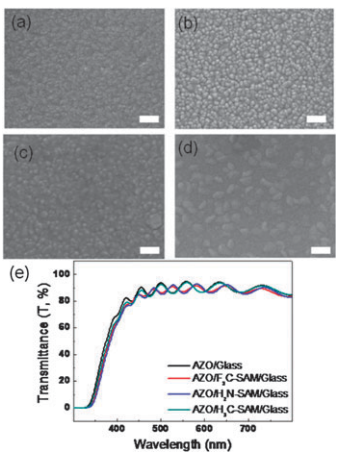

Fig. 3 SEM images of AZO films ($t \approx$ 120 nm) deposited on (a) bare glass, (b) F_3C–SAM, (c) H_3C–SAM, and (d) H_2N–SAM modified glass substrates. Scale bar is 100 nm. (e) Optical transmittance for AZO films ($t \approx$ 920 nm) deposited on various SAM modified glass substrates.

Table 1 Summary of the electrical properties of various AZO films. Data of (002) peak shift and peak intensity ratio of (002)/(103) from XRD analysis are also given along with the atomic percentage of dopants (Al) for a better comparison

AZO on various substrates	XRD analysis		At % of Al	Carrier density,[a] n ($\times 10^{21}$ cm^{-3})	Hall mobility, μ/cm^2 V^{-1} s^{-1}	Resistivity, ρ (10^{-4} Ω cm)	Sheet resistance[a]/ Ω/□
	(002) Peak shift/°	(002)/(003) Peak intensity ratio					
Glass	—	—	2.32	7.18	8.55	9.85	11.2
F_3C–SAM/glass	0.30	1.38	2.39	8.22	14.55	6.83	7.4
H_3C–SAM/glass	0.19	1.18	2.07	5.45	15.15	7.96	9.0
H_2N–SAM/glass	0.40	0.12	2.18	6.59	12.26	7.86	8.6

[a] The electrical properties were measured by the van der Pauw method. Data were collected for AZO films with $t \approx 920$ nm.

results which clearly exhibit the polycrystalline nature of AZO films on SAM modified glass substrates. Unlike the electrical properties of ITO films, the changes in the texture of the AZO films have little impact on their electrical behavior.[10,18] However, dopants concentration and their positions in the crystal lattice dominate the electrical properties. Table 1 summarizes the electrical properties of various AZO films. It is evident that all AZO films show similar electrical behavior with low sheet resistance (7–9 Ω/□), except the AZO film on a bare glass substrate which has marginally high resistance (11.2 Ω/□). Similarly, resistivity of the AZO film on a bare glass substrate (9.85×10^{-4} Ω cm) is higher than the AZO films on F_3C–SAM (6.83×10^{-4} Ω cm), H_3C–SAM (7.96×10^{-4} Ω cm), and H_2N–SAM (7.86×10^{-4} Ω cm). It is apparent from Table 1 that both % doping and (002)/(103) peak intensity ratio play a crucial role in electrical properties.[5] Since the AZO film on a F_3C–SAM modified glass substrate shows the maximum atomic % of aluminium content and the highest value of (002)/(103) peak ratio, it has the lowest sheet resistance and resistivity. This is in good agreement with previous reports that crystallographic orientation and % of aluminium content both play crucial roles in the electrical properties of AZO films.[5] However, strong (002) preferential orientation is not the only criterion for low resistivity of AZO films. For example, an AZO film on a H_2N–SAM modified glass substrate also shows low resistivity. Evidently, (103) orientation has a significant effect on the electrical properties of AZO films.[15] It is noteworthy to mention that resistivity and sheet resistance of the AZO film deposited on a H_3C–SAM terminated glass substrate are relatively high. Nonetheless, sheet resistance and resistivity values of current AZO films on different SAMs modified glass substrates are comparable to the results reported earlier for AZO films deposited by magnetron sputtering at 250 °C.[17] All the above AZO films show good optical transparency with ~85% transmittance in the range 380–800 nm (Fig. 3e).[2]

In summary, we have demonstrated that variation of the polarity of SAMs has dramatic impact on the gas phase crystal growth. This study will become an important part in many electronic device fabrications, especially with the recent developments in the ultra-thin film techniques,[19] where delicate alteration of crystalline structure of TCO films is necessary for the desired physical properties while avoiding adverse treatments.

This work was supported by Academia Sinica (nano-2394) and National Science Council (98-2113-M-011-002-MY2). The authors also thank Prof. L.-S. Hong and Prof. T. C.-K. Yang.

Notes and references

1 J. E. Costellano, in *Handbook of Display Technology*, Academic Press, New York, 1992.
2 H. Kim, C. M. Gilmore, J. S. Horwitz, A. Piqué, H. Murata, G. P. Kushto, R. Schlaf, Z. H. Kafafi and D. B. Chrisy, *Appl. Phys. Lett.*, 2000, **76**, 259.
3 X. Jiang, F. L. Wong, M. K. Fung and S. T. Lee, *Appl. Phys. Lett.*, 2003, **83**, 1875.
4 G. B. Murdoch, S. Hinds, E. H. Sargent, S. W. Tsang, L. Mordoukhovski and Z. H. Lu, *Appl. Phys. Lett.*, 2009, **94**, 213301.
5 M. Ohyama, H. Kozuka and T. Yoko, *J. Am. Ceram. Soc.*, 1998, **81**, 1622.
6 J. F. Chang and M. H. Hon, *Thin Solid Films*, 2001, **386**, 79.
7 N. W. Schmidt, T. S. Totushek, W. A. Kimes, D. R. Callender and J. R. Doyle, *J. Appl. Phys.*, 2003, **94**, 5514.
8 C. Oliveira, I. Rebouta, T. de Lacerda-Arôso, S. Lanceros-Mendez, T. Viseu, C. J. Tavares, J. Tovar, S. Ferdov and E. Alves, *Thin Solid Films*, 2009, **517**, 6290.
9 J. Anguita, M. Twaites, B. Holton, P. Hockley, S. Rand and S. Haughton, *Plasma Processes Polym.*, 2007, **4**, 48.
10 J. Sharma, H.-C. Chang and Y. Tai, *Langmuir*, 2010, **26**, 8251.
11 A. Ulman, *Chem. Rev.*, 1996, **96**, 1533; C. Yan, M. Zharnikov, A. Gölzhäuser and M. Grunze, *Langmuir*, 2000, **16**, 6208; Y. Tai, A. Shaporenko, W. Eck, M. Grunze and M. Zharnikov, *Appl. Phys. Lett.*, 2004, **85**, 6257; C. L. Rhodes, S. Lappi, D. Fischer, S. Sambasivan, J. Genzer and S. Franzen, *Langmuir*, 2008, **24**, 433.
12 B. C. Bunker, P. C. Rieke, B. J. Tarasevich, A. A. Campbell, G. E. Fryxell, G. L. Graff, L. Song, J. Liu, J. W. Virden and G. L. McVay, *Science*, 1994, **264**, 48; J. Küther and W. Termel, *Chem. Commun.*, 1997, 2029; J. Küther, G. Nelles, R. Seshadri, M. Schaub, H. J. Butt and W. Termel, *Chem.–Eur. J.*, 1998, **4**, 1834; M. Aslam, S. Pethkar, K. Bandopadhya, I. S. Mulla, S. R. Sainkar, A. B. Mandal and K. Vijayamohanan, *J. Mater. Chem.*, 2000, **10**, 1737.
13 B.-Y. Oh, M.-C. Jeong, W. Lee and J.-M. Myoung, *J. Cryst. Growth*, 2005, **274**, 453.
14 A. D. Trolio, E. M. Bauer, G. Scavia and C. Veroli, *J. Appl. Phys.*, 2009, **105**, 113109.
15 G. Xiao-Yong, L. Qing-Geng, F. Hong-Liang, L. Yu-Fen and L. Jing-Xiao, *Thin Solid Films*, 2009, **517**, 4684.
16 K. H. Kim, K. C. Park and D. Y. Ma, *J. Appl. Phys.*, 1997, **81**, 7764.
17 E.-G. Fu, D.-M. Zhuang, G. Zhang, Z. Ming, W.-F. Yang and J.-J. Liu, *Microelectron. J.*, 2004, **35**, 383.
18 R. B. H. Tahar and N. B. H. Tahar, *J. Appl. Phys.*, 2002, **92**, 4498.
19 X. Liang, M. Yu, J. Li, Y.-B. Jiang and A. W. Weimer, *Chem. Commun.*, 2009, 7140.